applied sciences

MDPI

Article

Deposition of Copper on Polyester Knitwear Fibers by a Magnetron Sputtering System. Physical Properties and Evaluation of Antimicrobial Response of New Multi-Functional Composite Materials

Marcin H. Kudzin *, Anna Kaczmarek, Zdzisława Mrozińska and Joanna Olczyk

Lukasiewicz Research Network -Textile Research Institute, Brzezinska 5/15, 92-103 Lodz, Poland; akaczmarek@iw.lodz.pl (A.K.); zmrozinska@iw.lodz.pl (Z.M.); olczyk@iw.lodz.pl (J.O.)

* Correspondence: kudzin@iw.lodz.pl; Tel.: +48-42-6163121

Received: 17 August 2020; Accepted: 1 October 2020; Published: 7 October 2020

Abstract: In this study, copper films were deposited by magnetron sputtering on poly(ethylene terephthalate) knitted textile to fabricate multi-functional, antimicrobial composite material. The modified knitted textile composites were subjected to microbial activity tests against colonies of Gram-positive (*Staphylococcus aureus*) and Gram-negative (*Escherichia coli*) bacteria and antifungal tests against *Chaetomium globosum* fungal molds species. The prepared samples were characterized by UV/VIS transmittance, scanning electron microscopy (SEM), tensile and filtration parameters and the ability to block UV radiation. The performed works proved the possibility of manufacturing a new generation of antimicrobial textile composites with barrier properties against UV radiation, produced by a simple, zero-waste method. The specific advantages of using new poly(ethylene terephthalate)-copper composites are in biomedical applications areas.

Keywords: knitwear textile; poly(ethylene terephthalate); polymer functionalization; copper; composites; magnetron sputtering; antibacterial activity; antifungal activity

1. Introduction

Poly(Ethylene Terephthalate) (PET), due to its physicochemical and technical attributes (high uniformity, mechanical strength, permeability to gases, transparency and resistance against UV and chemicals), presents a multifunctional polymer [1–3] widely engaged in various applications ranging from a production of containers and packaging [4], through textiles [5–8], the health care polymeric materials [9–12] and concrete components [13] to flexible electronic device applications [14].

However, the lack of antibacterial properties with unsatisfactory biocompatibility and functionality of PET frequently limits its use in some industrial and medical fields, especially in biomedical device and filtration membrane applications [15]. Moreover, due to its own porosity PET is conducive to microbial adhesion and subsequent bacteria colonization [16]. Therefore, for improvement of antimicrobial properties PET was subjected to several surface modification technologies [17,18], the majority based on functionalization [19,20], grafting [21–28], surface topography modification [29–33], coating [34–37] and their combinations [38–40].

Of substantial importance in the field of antimicrobial PET are its composites, equipped with antibacterial organic additivities (mainly chitosan and antibiotics [21,22,41–50]). Thus, antimicrobial hybrids of PET-organic biocides can be represented by PET-Chitosan [21,22,41], PET-Chitosan/hyaluronic acid [42–44], PET-Antibiotics (e.g., rifampin [45]; cephalosporin [46]; gentamicin [47], tetracycline [48]; chlorhexidine [49] or daptomycin [50]).

Because of increasing demand for effective antimicrobials combating bacterial cross-infections and infectious diseases [51], metals and salts deposited over polymers became a valuable alternative to traditional antibiotics [52–59]. In hybrids PET-inorganic bactericides representative are: PET-Ag nanoparticles [60–67], PET-silver salts [68,69], PET-TiO_2 [70–73], PET-Zn/ZnO_2 [74–77] and/or PET-Au [78]. In the set of PET-metal hybrids only a few PET-Cu hybrids have been reported [79–82].

Between various inorganic bactericides of medicinal interest growing attention is focusing on copper and its salts (over 5200 documents on antibacterial activity of copper abstracted by Scopus) [83], due to their low costs and easy preparation [84–86] as well as an antimicrobial efficiency [87–96]. The antibacterial activity of the copper metallic surface is regarded to act by two supplemental mechanisms—surface–surface interaction of copper and bacteria (contact killing) [93] and/or surface oxidation of copper with the subsequent release of antibacterial cupric ions (e.g., [93,94]).

Polymer-copper composites have been formed by a number of various methods, [95–98], including magnetic sputtering method: a simple and ecofriendly method, allowing deposition of the required amount of deposited metal in function of the time applied [99–101].

As a part of our research program directed on biologically active functionalized phosphonates [102,103] and biofunctionalization of textile materials [104–106] we present the preparation and physico-chemical and biological properties of the PET-Cu polymer hybrid.

The aim of this work was to modify the surface of the polyethylene terephthalate knitwear textile with copper, using the DC (Direct Current) magnetron sputtering method and fabrication of a new antimicrobial, multi-functional composite material.

As far as pretreatment and finishing of textile fabrics are concerned, plasma technologies are currently increasingly replacing wet chemical processes. For instance, Shahidi et al. [107] applied magnetron sputtering to modify the woven cotton fabrics with Cu. The authors highlighted that magnetron sputtering is a simple, environmentally friendly and time-saving method in comparison to the conventional process, which requires the use of a detergent, metallic salts and at least three baths (more than 100 min). In turn Badaraev et al. [108] pointed out that magnetron sputtering allows one to avoid the high costs associated with the synthesis of nanoparticles applied for the modification of the textile surface and thus, offers a resource-efficient method for producing textiles with antimicrobial properties. Taking into consideration that the modification of textile materials using magnetron sputtering does not require the use of any chemicals and may be realized in a single process cycle in a single industrial installation, as indicated by Gorberg et al. [109], it may be considered as simple technique. Additionally, magnetron sputtering is not associated with any toxic emission to the environment or contamination production. Therefore, this method may be considered as an eco-friendly and zero-waste one.

2. Materials and Methods

2.1. Materials

- Knitted textile, qualitative composition: polyester—polyethylene terephthalate (95%*w*/*w*), elastane—polyether-polyurea copolymer (5%*w*/*w*), weave: interlock right, basic weight (GSM): 230 g/m^2; assigned as PETE (polyethylene terephthalate-elastane, for structures see Figure 1) (IW, Lodz, Poland). The size of the textile sample was 300 mm × 150 mm.
- The copper target (Testbourne Ltd., Basingstoke, UK) with 99.99% purity. The size of the target was equal to 798 × 122 × 6 mm.
- Bacterial and Fungal Strains were purchased from Microbiologics (St. Cloud, MN, USA): *Escherchia coli* (ATCC 25922), *Staphylococcus aureus* (ATCC 6538) and fungal strains: *Chaetomium globosum* (ATCC 6205).

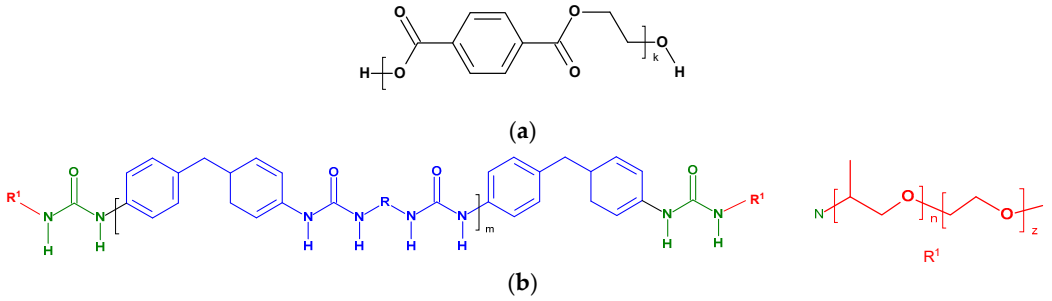

Figure 1. The structures of polymer components of polyethylene terephthalate-elastane (PETE). (**a**) Polyethylene Terephthalate (PET) (k, m, n, z-the degree of polymerization). (**b**) Elastane (EA) (ABA polyether–polyurea–polyether block copolymer; R= linear, cyclic or aromatic diamine chain exchanger; m = 29; z = 6) according to Locatelli et al. [110].

2.2. Methods

2.2.1. Magnetron Sputtering

The knitted PETE samples were modified using a DC magnetron sputtering system produced by P.P.H. Jolex s. c. (Czestochowa, Poland), schematically presented in Figure 2.

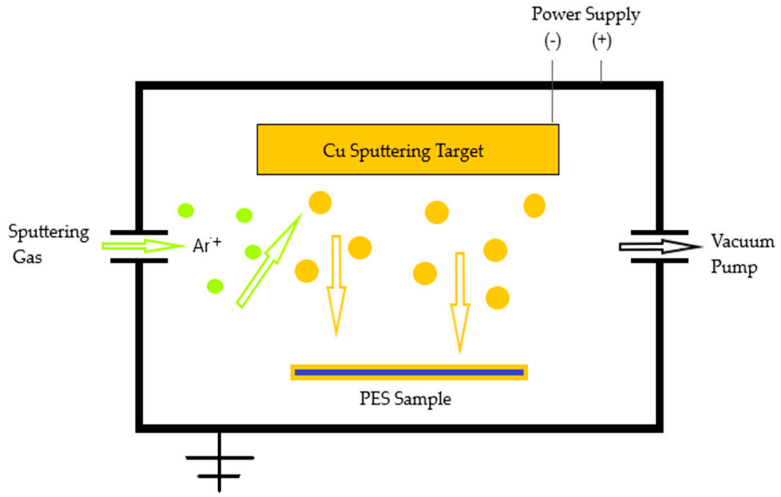

Figure 2. The schematic diagram of applied DC magnetron sputtering system.

The apparatus was developed for the Lukasiewicz Research Network—Textile Research Institute in Lodz, Poland—for the purpose of the project Envirotex—PO IG no. 01.03.01-00-006/08 co-financed from the funds of European Regional Development Fund within the framework of the Operational Programme Innovative Economy 2007–2013. It allows the semi-continuous deposition of metallic coatings on different fabrics (up to 60 cm wide).

The deposition of coatings was carried out in the atmosphere of argon, the distance between a copper target and the sputtering substrate was equal to 15 cm, the applied powers varied from 350 to 1000 W. The established optimal sputtering conditions were: the power discharge—700 W; the time of deposition—10 min; the resulting power density—0.72 W/cm^2 and the working pressure 2.0×10^{-3} mbar. The applied parameters were chosen on the basis of the previous research concerning the deposition of copper on the Polylactide (PLA) nonwoven fabrics. A preliminary study was performed for the purpose of another publication, which has been recently published [111]. In order to choose the appropriate deposition parameters, the authors varied the sputtering power of the magnetron target from 350 up to 1000 W. At the same time, the sputtering time was changed from 10 to 30 min. The upper limit of the applied power was set as a result of our previous experiments showing

that higher values of power have destructive effect on the PLA substrate. The preliminary analysis of antimicrobial activity was carried out for the obtained samples. The results exhibited no antibacterial and antifungal effect for the sputtering power lower than 700 W. Taking into consideration the possible cytotoxicity of copper, the authors decided to choose the minimal sputtering power for which the antimicrobial activity was observed for further research. This allows us to minimize the content of copper and thus, minimizes the risk of cytotoxicity. In order to enable the comparison of results obtained for different materials, the authors decided to apply the same deposition parameters for the PETE substrate as for the PLA substrate. Since for the PLA nonwovens the observed antibacterial activity did not vary substantially between the samples subjected to 10 and 30 min of copper deposition, the authors decided to choose the lower deposition time in order to further limit the Cu content. Therefore, the final deposition parameters applied in this work were established at 700 W and 10 min for each side of the substrate.

In order to vary the copper content in the PETE-Cu$^{(0)}$, composites two different deposition variants were applied, namely: 10 min single-sided deposition of copper on PETE (sample name: PETE-Cu$^{(0)}$-1) and 20 min two-sided deposition of PETE (10 min for the upper and 10 min for the lower side of the sputtering fabric; sample name: PETE-Cu$^{(0)}$-2; PETE-Cu$^{(0)}$-2.1 and PETE-Cu$^{(0)}$-2.2).

2.2.2. SEM/EDS—Scanning Electron Microscopy/Energy-Dispersive X-ray Spectroscopy

The microscopic analysis of fibers was performed on a Tescan Vega 3 scanning electron microscope (Tescan Analytics, Brno, Czech Republic) with the EDS (Oxford Instruments, Abingdon, UK) X-ray micro analyzer. The SEM microscopic examination of the surface topography was carried out in a high vacuum using the energy of the probe beam 20 keV. The layer of gold (approx. 3.5 nm), as a conductive substance, was sputtered on the samples before SEM analysis using a Quorum Technologies Ltd. (Lewes, UK) vacuum dust extractor. The instrument is fitted with a 57 mm diameter quick-change magnetron sputter target. Gas supplies: Argon. Vacuum: 5×10^{-5} mbar. Magnifications of SEM applied were in the range from 500× to 20,000×. The performance of an EDS system was evaluated by measuring the resolution of a known set of elemental standards (Oxford Instruments, Abingdon, UK) in line with the ISO 15632:2012 [112].

2.2.3. FAAS—Flame Atomic Absorption Spectrometry

For the determination of copper content in PETE-Cu$^{(0)}$, samples were assessed by prior sample mineralization (Figure 3), using a single-module Magnum II microwave mineralizer from Ertec (Wroclaw, Poland), followed by the determination of copper (II) ions by atomic absorption spectrometry with flame excitation using the Thermo Scientific Thermo Solar M6 (LabWrench, Midland, ON, Canada) spectrometer equipped with a 100 mm titanium burner, coded lamps with a single-element hollow cathode, background correction: D2 deuterium lamp.

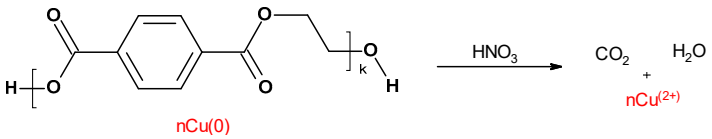

Figure 3. Mineralization of PETE-Cu$^{(0)}$ (k-the degree of polymerization).

The total copper content of the sample M [mg/kg; ppm] was calculated according to the formula [113]:

$$M = \frac{C_i \times V}{m_i} \text{ [mg kg]}$$

here:

C_i—metal concentration in the tested solution [mg/L];
m_i—mass of the mineralized sample [g];

V—volume of the sample solution [mL].

2.2.4. UV-VIS Analysis and Determination of the Protective Properties Against UV Radiation

Changes of the physical properties as transmittance [%T] of samples occurring during modifications were assessed using a double beam Jasco V-550 UV-VIS spectrophotometer (Jasco, Tokyo, Japan) with an integrating sphere attachment in the range 200–800 nm. The same apparatus was used to determine the Ultraviolet Protection Factor (UPF) of samples, according to EN 13758-1:2002 standard [114], using the formula:

$$UPF = \frac{\int_{290}^{400} E(\lambda)\varepsilon(\lambda)d(\lambda)}{\int_{290}^{400} E(\lambda)\varepsilon(\lambda)T(\lambda)d(\lambda)}$$

where:

$E(\lambda)$—the solar irradiance;
$\varepsilon(\lambda)$—the erythema action spectrum (measure of the harmfulness of UV radiation for human skin);
$\Delta\lambda$—the wavelength interval of the measurements;
$T(\lambda)$—the spectral transmittance at wavelength λ.

The UPF value of the samples was determined as the arithmetic mean of the UPF values for each of the samples, reduced by the statistical value depending on the number of measurements performed, at a confidence interval of 95%.

2.2.5. Filtration Parameters

Air permeability of the PETE knitted fabrics and PETE-Cu$^{(0)}$ composites was determined according to the EN ISO 9237:1998 standard [115]. An FX 3300 TEXTEST AG (Klimatest, Wrocław, Poland) permeability tester was applied. During the test, air at a pressure of 100 Pascal and 200 Pascal was passed through a fabric area of 20 cm^2. Air permeability was determined as an average of 10 measurements for each type of sample.

2.2.6. Tensile Testing

Tensile testing of the PETE knitted fabrics and PETE-Cu$^{(0)}$ composites was performed in accordance with the EN ISO 10319:2015 standard [116]. A H5KS (Hounsfield, Redhill, UK) testing machine was used. The cross-head stretching speed was equal to 100 mm/min, the support spacing was 100 mm, while the width of the sample was 50 mm. The initial pressure force was set at 0.5 N. Measurements were carried out for both longitudinal and horizontal directions.

2.2.7. Thickness

Thickness measurements of the PETE knitted fabrics and PETE-Cu$^{(0)}$ composites were conducted in accordance with the EN ISO 5084:1999 standard [117]. The thickness of each sample was calculated as an average of 10 measurements. The area of the tested samples was equal to 20 cm^2. The measurements were performed using a GM-70 thickness gauge (IW, Lodz, Poland) at the pressure of 1 kPa.

2.2.8. Thermal Resistance, Steam Resistance and Steam Permeability

Thermal resistance, steam resistance and steam permeability of the PETE knitted fabrics and PETE-Cu$^{(0)}$ composites were measured according to the EN ISO 11092:2014-11 [118] using a KONTECH apparatus (IW, Lodz, Poland). The application of this measurement technique is restricted to a maximum thermal resistance and water-vapour resistance e.g., 2 m^2·K/W and 700 m^2·Pa/W respectively. The airflow speed was set to 1.0 m/s.

2.2.9. Bacterial Activity

The antibacterial activity of PETE-Cu$^{(0)}$ composites was tested according to the PN-EN ISO 20645:2006 [119] against a colony of Gram-negative bacteria (*Escherchia coli*, ATCC 25922) and Gram-positive bacteria (*Staphylococcus aureus*, ATCC 6538), using the agar diffusion method of Muller Hinton. The test was initiated by pouring agar on to sterilized Petri dishes and it was allowed to solidify. The surfaces of agar media were inoculated by overnight broth cultures of bacteria (ATCC 25922: 1.2×10^8 CFU/mL, ATCC 6538: 1.7×10^8 CFU/mL) and kept at 4 °C before analysis. In order to establish the bacterial concentration inside the overnight culture the assessment of turbidity of bacterial suspension as well as the culture method were used. The density of the bacterial suspension was firstly determined using a calibrated densitometer. Then, using a series of ten-fold dilutions, the number of colonies grown on the plates was calculated from the appropriate dilutions and relevant calculations were made.

Discs of PETE-Cu$^{(0)}$ composites (10 mm) were placed onto the inoculated agar and incubated at 37 °C for 24 h. The diameter of the clear zone around the discs was measured as an indication of inhibition of the microbial species. Each side of the sample was tested in duplicate (four tests were performed for each sample). Simultaneously, the same tests were carried out for control samples—unmodified PETE samples.

2.2.10. Antifungal Activity

The procedure applied was partly identical with the procedure above. Thus, the antifungal activity of PETE-Cu$^{(0)}$ composites was tested according to PN-EN 14119:2005 [120] against a *Chaetomium globosum* (ATCC 6205). Discs of the tested PETE-Cu$^{(0)}$ composites (20 mm) were placed onto the inoculated with *Chaetomium globosum* fungal moulds species agar (pH:6.2) plates and incubated at 29 °C for 14 days. Both sides of PETE-Cu$^{(0)}$ composites were tested. The level of antifungal activity was assessed by examining the extent of fungal growth: in the contact zone between the agar and the specimen, on the surface of specimens and, if present, the extent of the inhibition zone around the specimen. All tests were carried out in duplicate. Simultaneously, the same tests were carried out for control samples (unmodified PETE).

3. Results and Discussion

3.1. SEM—Scanning Electron Microscopy

SEM micrographs of PETE fabrics and PETE-Cu$^{(0)}$ composites are presented in Figures 4 and 5, respectively.

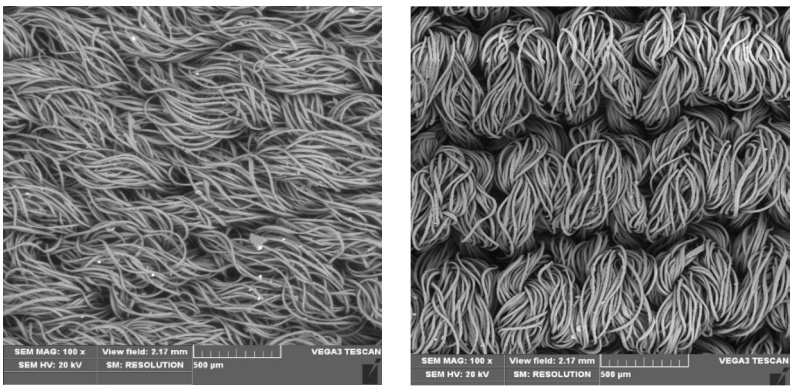

(**a**) (**b**)

Figure 4. *Cont.*

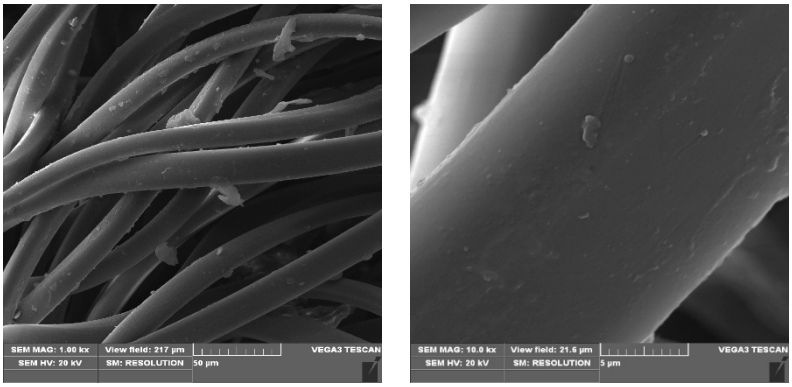

(**c**) (**d**)

Figure 4. Scanning electron microscopy images of the PETE knitted textile samples (unmodified), magnification: 100× ((**a**,**b**): right/left side of the knitted textile sample), 1000× (**c**), 10,000× (**d**).

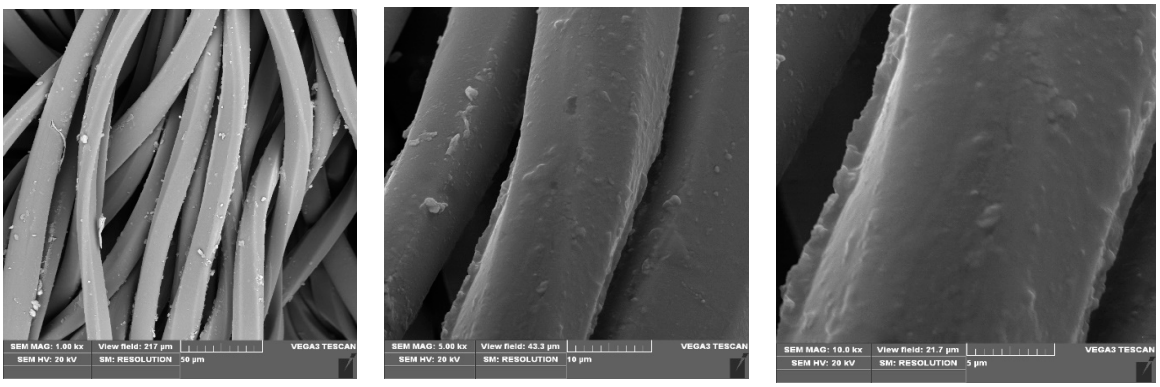

(**a**) (**b**) (**c**)

Figure 5. Scanning electron microscopy images of PETE-$Cu^{(0)}$-1 composite, magnification: 1000× (**a**), 5000× (**b**), 10,000× (**c**).

The SEM images of the unmodified PETE fabrics show parallel and uniform randomly oriented fibers (Figure 4a) with relatively smooth surfaces (Figure 4d). The average fiber diameter in the PETE knitwear sample was 15 ± 2 µm. The SEM images of the magnetron sputtering PETE-$Cu^{(0)}$-1 composite (Figure 5) show changes in the surface structure of the samples, uniformly distributed new surface coating layer on the entire of the fibers (Figure 5b,c). No damage or fiber cracks in the PETE-$Cu^{(0)}$ composites were observed (Figure 5b,c).

3.2. Copper Determination in PETE-$Cu^{(0)}$/Composites

Copper determination in PETE-$Cu^{(0)}$ composites was achieved using EDS spectroscopy (determination of surface located copper) and FAAS spectrometry (determination of bulk copper).

3.3. Copper Determination by Energy-Dispersive X-ray Spectroscopy EDS

Comparison of the EDS analyses of PETE and PETE-$Cu^{(0)}$ composites are presented in Table 1.

Table 1. The EDS analysis of elemental composition of PETE (C, O) and PETE-Cu$^{(0)}$ (C, O, Cu) composites.

	PETE		PETE-Cu$^{(0)}$ [a]					
			PETE-Cu$^{(0)}$-1 [a]					
			PETE-Cu$^{(0)}$-1.1 [c]			PETE-Cu$^{(0)}$-1.2 [c]		
Element	**C**	**O**	**C**	**O**	**Cu**	**C**	**O**	**Cu**
% [b,c]	61.8	37.8	19.90	4.40	75.60	61.40	38.30	-
Std. deviation	0.16	0.16	0.82	0.06	0.79	0.14	0.16	-
	PETE		**PETE-Cu$^{(0)}$-2 [a]**					
			PETE-Cu$^{(0)}$-2.1 [d]			**PETE-Cu$^{(0)}$-2.2 [d]**		
Element	**C**	**O**	**C**	**O**	**Cu**	**C**	**O**	**Cu**
% [b]	62.1	37.5	17.70	5.93	74.78	22.83	6.14	70.88
Std. deviation	0.16	0.16	1.70	0.45	0.26	1.47	0.71	2.20

[a] Assignments: PETE-Cu$^{(0)}$-1—one site a PETE sample copper sputtering deposition: PETE-Cu$^{(0)}$-1.1—upper site of the sample analysis; PETE-Cu$^{(0)}$-1.2—lower site of the sample analysis; PETE-Cu$^{(0)}$-2: two sites of a PETE sample copper sputtering deposition; PETE-Cu$^{(0)}$-2.1—upper site of the sample analysis; PETE-Cu$^{(0)}$-2.2—lower site of the sample analysis; [b] All results in percent by weight [%]; [c] Mean value of 3 measurements; [d] Mean value of 11 measurements.

The analyses of deposited sites of the PETE-Cu$^{(0)}$ composites performed for both one site as well as two sites modes of copper sputtering afforded close results for PETE-Cu$^{(0)}$-1.1 and PETE-Cu$^{(0)}$-2.1 and slightly different results were seen for PETE-Cu$^{(0)}$-2.2. Thus, for carbon: 19.9% (PETE-Cu$^{(0)}$-1.1), 17.70% (PETE-Cu$^{(0)}$-2.1) and 22.83% (PETE-Cu$^{(0)}$-2.2), respectively; for oxygen: 4.40% (PETE-Cu$^{(0)}$-1.1), 5.93% (PETE-Cu$^{(0)}$-2.1) and 6.14% (PETE-Cu$^{(0)}$-2.2), respectively; and for copper: 75.6% (PETE-Cu$^{(0)}$-1.1), 74.78% (PETE-Cu$^{(0)}$-2.1) and 70.88% (PETE-Cu$^{(0)}$-2.2), respectively.

These differences can be caused by the different morphology of both sides of the knitted PETE textile (weave: interlock right) used for the copper sputtering deposition [121], influencing on a type of deposited copper. The Flame Atomic Absorption Spectrometry results advocate for the proportional increase of deposition of copper during the deposition. We also consider the influence of the already-formed copper layer on the copper diffusion inside bulk during sputtering of the second side of the textile (PETE-Cu$^{(0)}$-2.2).

Is worth admitting that the distribution and penetration of the Cu atoms into the polymer beneath the interface, and the exact nature of the Cu–O–C bonds formed during polyarylamide PAMX D6 copper sputtering, are still unclear since Legois' work [122].

3.4. Copper Determination by Flame Atomic Absorption Spectrometry—FAAS

The results of copper content in PETE-Cu$^{(0)}$ composite samples determined by the FAAS method are listed in Table 2.

Table 2. Results of determination of copper content in PETE and PETE-Cu$^{(0)}$ composite samples by Flame Atomic Absorption Spectrometry (FAAS).

Sample Name	**Copper Deposition Time [min]**	**Copper Concentration Determined**		
		[g/kg]	**Percentage [%: g/100 g]**	**Molality [*m*: mmol/kg]**
PETE	-	0.026	0.003	0.0004
PETE-Cu$^{(0)}$-1	10	6.701	0.670	0.105
PETE-Cu$^{(0)}$-2	20	14.036	1.404	0.221

The results have been measured in triplicate and presented as a mean value with deviations approximately ±2%.

The results inform about the whole copper concentration in starting PETE knitwear fibers and PETE-Cu$^{(0)}$ composites. These revealed that composites are practically null of copper in the starting PETE (0.003: %; *m*: 0.0004) with only 0.7% to 1.4% of copper in PETE-Cu$^{(0)}$ composites; in detail there was 0.67% (0.105 molal) of copper in one side of the sputtered knitwear fibers PETE-Cu$^{(0)}$-1 and twice as high a copper concentration in the case of two-sided sputtering mode PETE-Cu$^{(0)}$-2 (140%; 0.221 molal).

Taking into account the results of copper determination in PETE-Cu$^{(0)}$-2.2 by EDS and in PETE-Cu$^{(0)}$-2 by FAAS it can be assumed that during sputtering of the second side of PETE-Cu$^{(0)}$-2 (PETE-Cu$^{(0)}$-2 → PETE-Cu$^{(0)}$-2.2) the diffusion of copper from the sputtering surface (PETE-Cu$^{(0)}$-2.2) into bulk of polymer occurs, and there is copper diffusion in the polymer, analogous to earlier works on PET metallization [123–125].

3.5. UV-VIS Analysis and Determination of the Protective Properties Against UV Radiation

Poly(ethylene terephthalate) is transparent for UV, undergoing itself a surface modification under deep UV irradiation (e.g., [126,127]). The importance of protection against ultraviolet radiation (UV) is increasing daily. Investigations on poly(ethylene terephthalate) fibers' protection against solar ultraviolet radiation (UVR) have been frequently undertaken (e.g., [128–130]). The property of UVR protection exhibited by PETE-Cu$^{(0)}$ composites was investigated using a UV spectrophotometer by measuring the transmittance of UV-rays through the fabrics.

Thus, the transmittance spectra [%T] of starting PETE knitted textile and PETE-Cu$^{(0)}$ composites in the range λ = 200–800 nm are presented in Figure 6.

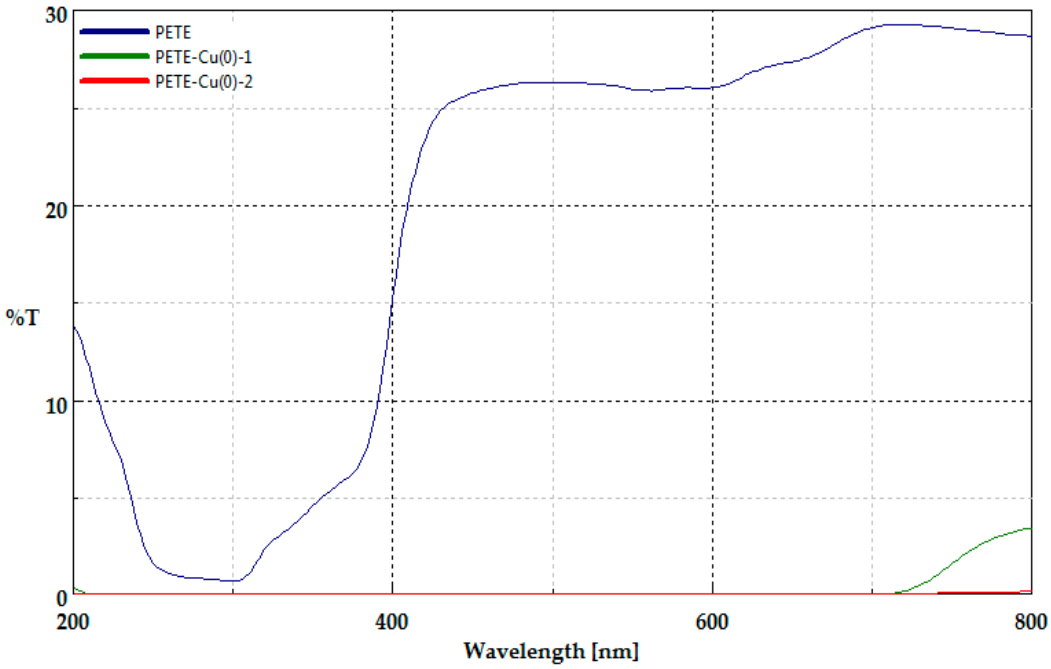

Figure 6. Comparison of transmittance spectra [%T] in the range λ = 200–800 nm of unmodified PETE knitted textile and PETE-Cu$^{(0)}$ composites (PETE-Cu$^{(0)}$-1, PETE-Cu$^{(0)}$-2).

As shown in Figure 6, the transmittance of UV-rays of the PETE fabrics, PETE-Cu$^{(0)}$-1 and PETE-Cu$^{(0)}$-2 composites were different in the wavelength range examined. Thus, the PETE transmittance curve exhibited a complexed shape, with a sharp decrease in the 200–250 nm range from ca 14%T to ca 1.5 %T, then a slow increase from 1.5% T (310 nm) to 7% T (380 nm), a rapid decrease to 26%T at 420 nm and the plateau region to 600 nm and a further gradual increase to 29%T at 700 nm with the plateau to 800 nm. The PETE-Cu$^{(0)}$-1composite exhibited null transmittance in the wavelength range 200 to 720 nm, with an increase to 3%T at the 720–800 nm range. The PETE-Cu$^{(0)}$-2composite exhibited null transmittance in the

full examined wavelength range 200 to 800 nm. As a result, the property of UVR protection of the both PETE-Cu$^{(0)}$ composites had improved significantly in almost the full wavelength range (excluding the 250–300 nm gap: 0%T for PETE-Cu$^{(0)}$ vs 1.5%T for PETE).

The transmittance (%T) spectra of PETE and PETE-Cu$^{(0)}$ composites in the range λ = 290–400 nm (UV A and UV B) are presented in Figure 7.

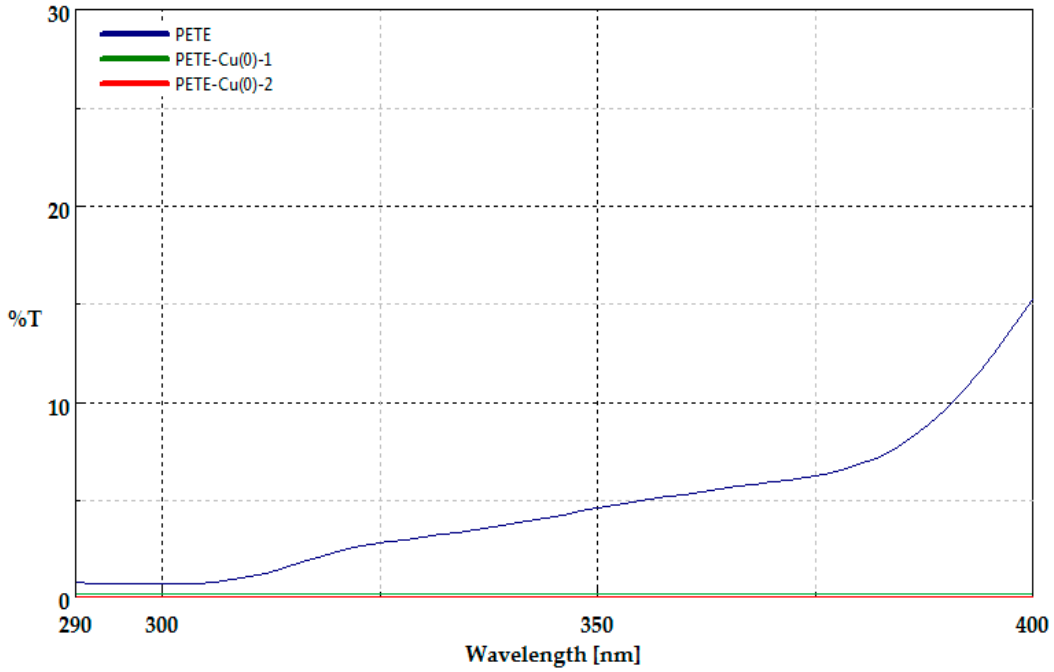

Figure 7. Comparison of transmittance spectra [%T] in the range λ = 290–400 nm of unmodified PETE knitted textile and PETE-Cu$^{(0)}$ composites (PETE-Cu$^{(0)}$-1, PETE-Cu$^{(0)}$-2).

On the basis of these transmittance measurements obtained for PETE knitted textile and PETE-Cu$^{(0)}$ composites at λ = 290–400 nm, corresponding UPF values have been calculated [114]. UPF values of PETE knitted textile and PETE-Cu$^{(0)}$ composites, calculated on the basis of transmittance measurements for λ = 290–400 nm (Figure 6), have been listed in the Table 3.

Table 3. Ultraviolet Protection Factor (UPF) values of PETE knitted textile and PETE-Cu$^{(0)}$ composites.

Parameter	PETE	PETE-Cu$^{(0)}$	
		PETE-Cu$^{(0)}$-1	PETE-Cu$^{(0)}$-2
UPF	37	>50	>50

The results have been measured in triplicate and presented as a mean value with. ±deviation approximately 2%.

These data revealed that both PETE-Cu$^{(0)}$ composites possess UPF$_{(PETE\text{-}Cu(0))}$ values > 50 in comparison with, UPF$_{(PETE)}$ values ~37 indicating that the magnetron sputtering modification performed imparts proper barrier properties of PETE knitted textile against UV radiation.

3.6. Technical Parameters

From several technical parameters affecting fabric behavior [131], we applied for PETE-Cu$^{(0)}$ composites utility verification analyses of filtration parameters, tensile strength, thickness as well as thermal resistance, steam resistance and steam permeability.

3.6.1. Filtration Parameters

Filtration parameters, expressed by the air permeability, present one of the major properties of textile materials and are governed by factors like the fabric structure, density, thickness and surface characteristics. The comparisons of air permeability of PETE-Cu$^{(0)}$ composites vs. PETE fabric are shown in Table 4. The obtained results indicated that the modification of PETE fabrics with copper coating moderately (16%–18%) decreases the air permeability from 65.5 mm/s to 54.5 mm/s at 100 Pa and from 147 mm/s to 123 mm/s at 200 Pa. Moreover, a slightly further reduction in the air permeability (51.8 mm/s at 100 Pa and 117 mm/s at 200 Pa) was observed for the sample coated with copper on both sides. Therefore, it may be concluded that the coating of PETE with copper minimally affected filtration parameters. Observed results may be associated with the changes of porosity of the sample due to the presence of the copper coatings on the surface.

Table 4. The air permeability of the unmodified PETE fabrics and PETE-Cu$^{(0)}$ composites, according to the EN ISO 9237:1998 [115].

Parameter		PETE	PETE-Cu$^{(0)}$	
			PETE-Cu$^{(0)}$-1	PETE-Cu$^{(0)}$-2
Average air permeability [mm/s], pressure decrease:	100 Pa	65.5 ± 1.5	54.5 ± 1.0	51.8 ± 1.0
	200 Pa	147.0 ± 4.0	123.0 ± 2.0	117.0 ± 2.0

The results have been measured in triplicate and presented as a mean value with. ±deviation approximately 3%.

The obtained results indicate 16%–18% decreases of the PETE air permeability accompanied its metallization (PETE→PETE-Cu$^{(0)}$-1: from 65.5 mm/s to 54.5 mm/s at 100 Pa and from 147 mm/s to 123 mm/s at 200 Pa and PETE→PETE-Cu$^{(0)}$-2: from 65.5 mm/s to 51.8 mm/s at 100 Pa and from 147 mm/s to 117 mm/s at 200 Pa, respectively) and 4%–5% decrease between air permeability PETE-Cu$^{(0)}$-1 and PETE-Cu$^{(0)}$-2 (from 54.5 to 51.8 at 100 Pa and from 123 to 117 at 200 Pa, respectively). These results may be associated with changes of porosity of the samples caused by formation of copper layers on the PETE surface during sputtering process (PETE → PETE-Cu$^{(0)}$-1 → PETE-Cu$^{(0)}$-2).

3.6.2. Tensile Strength

The results of tensile testing, i.e., tensile strength [kN/m] and elongation at maximum load [%], of PETE fabric and PETE-Cu$^{(0)}$ composites, determined in longitudinal and horizontal modes, are listed in Table 5.

Table 5. The results of tensile strength test of the unmodified PETE fabrics and PETE-Cu$^{(0)}$ composites, in accordance with the EN ISO 10319:2015 [116].

Parameter	PETE		PETE-Cu$^{(0)}$			
			PETE-Cu$^{(0)}$-1		PETE-Cu$^{(0)}$-2	
	Longitudinal	Horizontal	Longitudinal	Horizontal	Longitudinal	Horizontal
Tensile strength [kN/m]	7.0 ± 0.26	6.2 ± 0.10	7.8 ± 0.20	6.0 ± 0.52	7.6 ± 0.14	6.0 ± 0.26
Elongation at maximum load [%]	375 ± 9.35	421 ± 13.7	403 ± 6.76	405 ± 20.1	396 ± 6.75	413 ± 24.7

The results have been measured in triplicate and presented as a mean value.

The results presented opposite tendencies regarding as well elongation determined for PETE and PETE-Cu(0) in longitudinal and horizontal modes. Thus, ca 10% increase of tensile strength in longitudinal mode for PETE-Cu$^{(0)}$ in comparison with starting PETE fibre (7.8–7.6 vs 7.0 [kN/m]) is accompanied by corresponding ca 3% decrease in horizontal mode (6.0 vs 6.2 [kN/m]), respectively. At the same time, the differences of tensile strengths, measured for PETE-Cu$^{(0)}$-1 and PETE-Cu$^{(0)}$-2 in both modes are negligible.

Similarly, the elongation at maximum load increases ca 6% from 375% for PETE to 396%–403% for PETE-Cu$^{(0)}$ fabrics in longitudinal mode and decreases ca 5% from 421% for PETE to 405%–413% for PETE-Cu$^{(0)}$ fabrics in horizontal mode, respectively. At the same time, the differences in the elongations at maximum load, measured for PETE-Cu$^{(0)}$-1 and PETE-Cu$^{(0)}$-2 are negligible (lay in error limit).

3.6.3. Thickness

The data of thickness of the unmodified PETE fabrics and PETE-Cu$^{(0)}$ composites are listed in Table 6. These data displayed negligible differences with the average values of measured thickness at 1 kPa in the range of 0.66–0.67 mm.

Table 6. Thickness of the unmodified PETE fabrics and PETE-Cu$^{(0)}$ composites, in accordance with the EN ISO 5084:1999 [117].

Parameter		PETE	PETE-Cu$^{(0)}$	
			PETE-Cu$^{(0)}$-1	PETE-Cu$^{(0)}$-2
Average thickness [mm]	1 kPa	0.66 ± 0.02	0.67 ± 0.02	0.67 ± 0.02

The results have been measured in triplicate and presented as a mean value, estimated to two decimal point.

3.6.4. Thermal Resistance

The measured thermal resistance, steam resistance and steam permeability of PETE fabric and PETE-Cu$^{(0)}$ composites are listed in Table 7.

Table 7. Thermal resistance, steam resistance and steam permeability of the unmodified PETE fabrics and PETE-Cu$^{(0)}$ composites, according to the EN ISO 11092:2014-11 [118].

Parameter	PET	PETE-Cu$^{(0)}$	
		PETE-Cu$^{(0)}$-1	PETE-Cu$^{(0)}$-2
Thermal resistance [m^{2}K/W]	0.004	0.007	0.009
Steam resistance [m^{2}Pa/W]	2.770	2.820	3.240
Steam permeability [g/m^{2}Pah]	0.537	0.528	0.459

The results have been measured in triplicate and presented as a mean value, estimated to three decimal points.

The obtained results of thermal resistance exhibited a 1.75–2.25 fold increase of PETE-Cu$^{(0)}$ composites in comparison with starting PETE fabrics, namely from 0.004 m^{2}K/W for PETE to 0.007 m^{2}K/W for PETE-Cu$^{(0)}$-1 (the one-side metaled sample) and 0.009 m^{2}K/W for PETE-Cu$^{(0)}$-2 (the sample coated on both sides), respectively.

The steam resistance [m^{2}Pa/W] of PETE-Cu$^{(0)}$ composites exhibited ca 2%–17% increase in comparison with starting PETE fabrics, namely 2% increase (from 2.770 for PETE to 2.82 for PETE-Cu$^{(0)}$-1) and a 17% increase for PETE-Cu$^{(0)}$-2 (from 2.770 for PETE to 3.24 for PETE-Cu$^{(0)}$-2), respectively.

The steam permeability [g/m^2 Pah] of PETE-Cu$^{(0)}$ composites exhibited ca 2%–15% decrease in comparison with starting PETE fabrics, namely a 2% decrease (from 0.537 for PETE to 0.528 for PETE-Cu$^{(0)}$-1) for PETE-Cu$^{(0)}$-1 and a 15% decrease for PETE-Cu$^{(0)}$-2 (from 0.537 for PETE to 0.459 for PETE-Cu$^{(0)}$-2), respectively.

Recapitulating, the metallization of PETE fabrics increased the thermal resistance and steam resistance of obtained composites PETE-Cu$^{(0)}$ in comparison with the starting PETE fabrics in degrees dependent on the copper content. The opposite trend was observed for steam permeability, with a decrease of permeability increasing with the copper content.

3.7. Antimicrobial Properties

3.7.1. Antibacterial Activity

The PETE-Cu$^{(0)}$ samples were subjected to antimicrobial activity tests against Gram-negative *Escherichia coli* (ATCC11229) and Gram-positive *Staphylococcus aureus* (ATCC 6538). The inhibition experiment results for PETE and PETE-Cu$^{(0)}$ are presented in Figure 8.

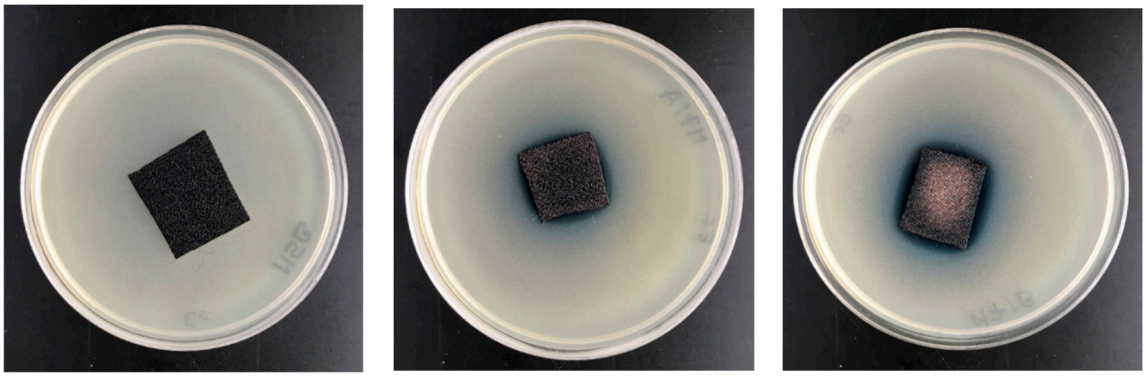

(**a**) (**b**) (**c**)

Figure 8. The PET samples coated with copper modifier antimicrobial activity tests. Inhibition zones of *Escherichia coli* bacterial growth on Petri dishes: (**a**) PETE, (**b**) PETE-Cu$^{(0)}$-1; (**c**) PETE-Cu$^{(0)}$-2.

The similar pictures have been obtained for PETE and PETE-Cu$^{(0)}$ against *Staphylococcus aureus* species.

The results of tests on the antibacterial activity of PETE-Cu$^{(0)}$ composites against *Escherichia coli* and *Staphylococcus aureus* are illustrated in Table 8.

Table 8. Results of tests on the antibacterial activity of PETE-Cu$^{(0)}$ composites, procedure in accordance with the EN ISO 20645:2006 [119].

Sample Name	Average Inhibition Zones for Bacterial Growth (mm)	
	E. coli	*S. aureus*
PETE	0	0
PETE-Cu$^{(0)}$-1	1	1
PETE-Cu$^{(0)}$-2	2	1

Concentration of inoculum (bacterial suspension) number of live bacteria: *E. coli*—CFU/mL = 1.2 × 108 and *S. aureus*—CFU/mL = 1.7 × 108.

The results revealed strong visible inhibition zones of bacterial growth on Petri dishes (Figure 8), and therefore proved antimicrobial protection of metallized surface of PETE-Cu$^{(0)}$ against representative Gram-negative (*Escherichia coli*) and Gram-positive (*Staphylococcus aureus*) bacteria (Table 8).

3.7.2. Antifungal Activity

Results of antifungal activity tests against a colony of *Chaetomium globosum* (ATCC 6205) of PETE fabrics and PETE-Cu$^{(0)}$ composites are illustrated in Figure 9 and listed in Table 9.

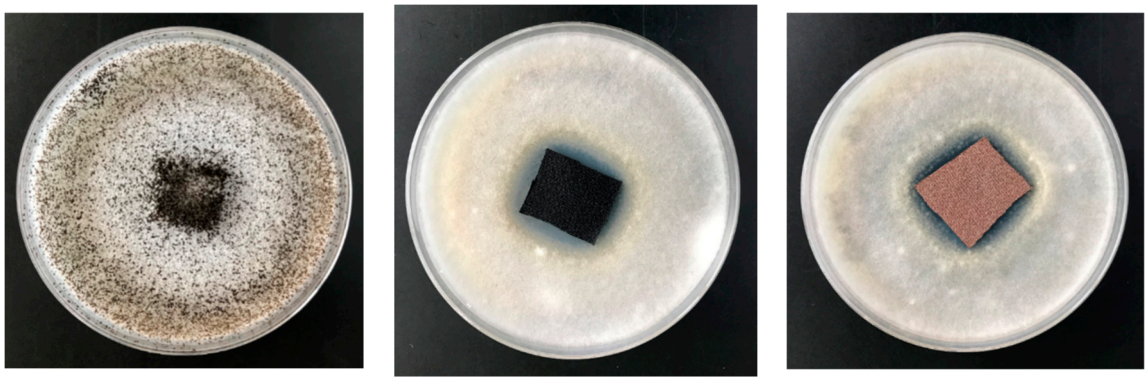

(**a**) (**b**) (**c**)

Figure 9. The PETE-Cu$^{(0)}$ composites antimicrobial activity tests against *Chaetomium globosum*. Inhibition properties of fungal growth on Petri dishes: (**a**) PETE, (**b**) PETE-Cu$^{(0)}$-1; (**c**) PETE-Cu$^{(0)}$-2.

Table 9. Results of tests on the antifungal activity of PETE-Cu$^{(0)}$ composites, procedure in accordance with the PN EN 14119: 2005 point 10.5 (B2) [120].

Sample Name	Fungal Average Inhibition Zone (mm)	
PETE	0	Visible growth on sample surface
PETE-Cu$^{(0)}$-1	3	No visible growth on sample surface
PETE-Cu$^{(0)}$-2	3	

Inoculum concentration, number of fungal spores in 1ml; [CFU/mL] = 2.2×10^6 (determined using a Thoma chamber).

The results revealed strong visible inhibition zones of fungal growth on Petri dishes (Figure 9), and therefore proved antifungal protection of metallized surface of PETE-Cu$^{(0)}$ against *Chaetomium globosum* (Table 9).

The results revealed that the unmodified PETE sample induced the strong fungal growth-covering of the entire surface of the control sample (Figure 9a). At the same time PETE-Cu$^{(0)}$composites equipped with copper layers/clusters on the composite surface provided antifungal properties for both—PETE-Cu$^{(0)}$-1 and PETE-Cu$^{(0)}$-2 composites.

4. Conclusions

(1) In this study a novel multi-functional, antimicrobial polyester-copper "hybrid" composite material, PETE-Cu$^{(0)}$, has been produced by one-step magnetron copper sputtering on PETE knitwear fibers (composed of poly(ethylene terephthalate) knitted textiles, PET (95%) and elastane, EA (5%)).

(2) The structural characterizations of the new PETE-Cu$^{(0)}$ polymer composites obtained, were characterized by Scanning Electron Microscopy (SEM) and UV/VIS transmittance. The chemical compositions of the PETE-Cu$^{(0)}$ composites obtained were achieved using Energy-Dispersive X-ray Spectroscopy, EDS (C, O, Cu surface analysis) and Atomic Absorption Spectrometry with Flame Excitation, FAAS (Cu content in the bulk).

(3) The application utility of the PETE-Cu$^{(0)}$ composites was established by determination of their technical parameters, including filtration parameters, tensile strength, thickness, thermal and steam resistance, steam permeability, the barrier properties against UV radiation and also antimicrobial tests against *Escherichia coli*, *Staphylococcus aureus* and *Chaetomium globosum* fungus species.

(4) SEM images of PETE-Cu$^{(0)}$ composites revealed that the applied magnetron sputtering of the starting PETE textile did not exhibit substantial destruction of the textile structure. Moreover, the described PETE-Cu$^{(0)}$ composites have shown improvement of the technical parameters, including air permeability and thermal and steam resistance. PETE-Cu$^{(0)}$ composites exhibited improvement of barrier properties against UV radiation in comparison with the unmodified PETE sample.

(5) Determined antimicrobial properties of PETE-$Cu^{(0)}$ composites revealed the significant antibacterial action of both PETE-$Cu^{(0)}$-1 as well as PETE-$Cu^{(0)}$-1 composites against *Escherichia coli*, *Staphylococcus aureus* and *Chaetomium globosum* fungus species.

(6). Recapitulating, the PETE-$Cu^{(0)}$ composites obtained, due to exhibited beneficial antibacterial and also technical properties, can find an application in a medical sector, for example, as a microbial barrier material.

Author Contributions: M.H.K. developed the concept and designed experiments, performed experiments, analyzed data and wrote the paper; A.K. performed experiments, analyzed the data and participated in the publication preparation; Z.M. performed experiments, analyzed the data and participated in the publication preparation; J.O. participated in the publication preparation. All authors have read and agreed to the published version of the manuscript.

Funding: This research was funded by the Polish Ministry of Science and Higher Education within statutory research work carried out at The Lukasiewicz Research Network -Textile Research Institute, Lodz, Poland.

Acknowledgments: This work was partly supported by National Science Centre, Poland via Grant: Miniatura 2, No. 2018/02/X/ST8/01775. The authors would like to thank Irena Kamińska, for performing SEM and EDS analyses and Agnieszka Lisiak-Kucińska, for providing the FAAS facilities.

Conflicts of Interest: The authors declare no conflict of interest.

References

1. Klare, H.; Reinisch, G. The structure and the properties of polyalkylene terephthalates (PATP). A review. *Polym. Sci. USSR* **1979**, *21*, 2727–2745. [CrossRef]
2. Pergal, M.V.; Balaban, M. *Poly(Ethylene Terephthalate): Synthesis and physicochemical properties In Polyethylene Terephthalate: Uses, Properties and Degradation*; Barber, N.A., Ed.; Nova Science Publishers, Inc.: Hauppauge, NY, USA, 2017; Chapter 1; pp. 1–102.
3. Fahim, A.M.; Farag, A.M.; Nawwar, G.A.M.; Yakout, E.S.M.A.; Ragab, E.A. Chemistry of tere-phthalate derivatives: A review. *Int. J. Environ. Waste Manag.* **2019**, *24*, 273–301. [CrossRef]
4. Beeva, D.A.; Borisov, V.A.; Mikitaev, A.K.; Ligidov, M.K.; Beev, A.A.; Barokova, E.B. Controlling the barrier properties of polyethylene terephthalate. A review. *Int. Polym. Sci. Technol.* **2015**, *42*, 45–52. [CrossRef]
5. Glenz, W. Polyethylene terephthalate (PET). *Kunststoffe Int.* **2007**, *97*, 50–54.
6. Matsuo, T. Fibre materials for advanced technical textiles. *Text. Prog.* **2008**, *40*, 87–121. [CrossRef]
7. Gong, X.; Chen, X.; Zhou, Y. Advanced weaving technologies for high-performance fabrics. In *High-Performance Apparel: Materials, Development, and Applications*; McLoughlin, J., Sabir, T., Eds.; Elsevier Ltd. (Woodhead Publishing 2018): Amsterdam, The Netherlands, 2017; Chapter 3; pp. 75–112.
8. Ma, Z.; Kotaki, M.; Yong, T.; He, W.; Ramakrishna, S. Surface engineering of electrospun polyethylene terephthalate (PET) nanofibers towards development of a new material for blood vessel engineering. *Biomaterials* **2005**, *26*, 2527–2536. [CrossRef]
9. Kenawy, E.R.; Worley, S.D.; Broughton, R. The chemistry and applications of antimicrobial polymers: A state-of-the-art review. *Biomacromolecules* **2007**, *8*, 1359–1384. [CrossRef]
10. Hadjizadeh, A.; Ajji, A.; Bureau, M.N. Preparation and characterization of NaOH treated micro-fibrous polyethylene terephthalate nonwovens for biomedical application. *J. Mech. Behav. Biomed. Mater.* **2010**, *3*, 574–583. [CrossRef]
11. Peck, M.; Gebhart, D.; Dusserre, N.; McAllister, T.N.; L'Heureux, N. The evolution of vascular tissue engineering and current state of the art. *Cells Tissues Organs* **2011**, *195*, 144–158. [CrossRef]
12. Jafari, S.; Hosseini Salekdeh, S.S.; Solouk, A.; Yousefzadeh, M. Electrospun polyethylene terephthalate (PET) nanofibrous conduit for biomedical application. *Polym. Adv. Technol.* **2020**, *31*, 284–296. [CrossRef]
13. Vishnu, A.; Mohana, V.; Manasi, S.; Ponmalar, V. Use of polyethylene terephthalate in concrete—A brief review. *Int. J. Civ. Eng. Technol.* **2017**, *8*, 1171–1176.
14. Chang, T.H.; Jung, Y.H.; Liu, D.; Mi, H.; Lee, J.; Gong, J.; Ma, Z. The applications of polyethylene terephthalate for RF flexible electronics. In *Polyethylene Terephthalate: Uses, Properties and Degradation*; Barber, N.A., Ed.; Nova Science Publishers, Inc.: Hauppauge, NY, USA, 2017; Chapter 2; pp. 103–153.

15. Tan, H.; Li, J.; Fu, Q. Preparation and characterization of non-fouling polymer brushes on poly(Ethylene terephthalate) film surfaces. In *Polymer Brushes: Substrates, Technologies, and Properties*; Mittal, V., Ed.; Taylor & Francis Group, LLC, CRC: Boca Raton, FL, USA, 2012; Chapter 5; pp. 91–114, ISBN 9780429107078. [CrossRef]
16. Wu, S.; Zhang, B.; Liu, Y.; Suo, X.; Li, H. Influence of surface topography on bacterial adhesion: A review (Review). *Biointerphases* **2018**, *13*, 060801. [CrossRef] [PubMed]
17. Adlhart, C.; Verran, J.; Azevedo, N.F.; Olmez, H.; Keinanen-Toivola, N.M.; Gouveia, I.; Melo, L.F.; Crijns, F. Surface modifications for antimicrobial effects in the healthcare setting: A critical overview. *J. Hosp. Infect.* **2018**, *99*, 239–249. [CrossRef] [PubMed]
18. Caykara, T.; Sande, M.G.; Azoia, N.; Rodrigues, L.R.; Silva, C.J. Exploring the potential of polyethylene terephthalate in the design of antibacterial surfaces. *Med. Microbiol. Immunol.* **2020**, *209*, 363–372. [CrossRef] [PubMed]
19. Swar, S.; Zajícova, V.; Rysova, M.; Lovetinska-Slamborová, I.; Volesky, L.; Stibor, I. Biocompatible surface modification of poly(ethylene terephthalate) focused on pathogenic bacteria:promising prospects in biomedical applications. *J. Appl. Polym. Sci.* **2017**, *134*, 1–11. [CrossRef]
20. Zhang, Z.; Zhao, Z.; Zheng, Z.; Liu, S.; Mao, S.; Li, X.; Chen, Y.; Mao, Q.; Wang, L.; Wang, F.; et al. Functionalization of polyethylene terephthalate fabrics using nitrogen plasma and silk fibroin/chitosan microspheres. *Appl. Surf. Sci.* **2019**, *495*, 143481. [CrossRef]
21. Huh, M.W.; Kang, I.-K.; Lee, D.H.; Kim, W.S.; Lee, D.H.; Park, L.S.; Min, K.E.; Seo, K.H. Surface characterization and antibacterial activity of chitosan-grafted poly(ethylene terephthalate) prepared by plasma glow discharge. *J. Appl. Polym. Sci.* **2001**, *81*, 2769–2778. [CrossRef]
22. Hu, S.G.; Jou, C.H.; Yang, M.C. Surface grafting of polyester fiber with chitosan and the antibacterial activity of pathogenic bacteria. *J. Appl. Polym. Sci.* **2002**, *86*, 2977–2983. [CrossRef]
23. Bedel, S.; Lepoittevin, B.; Costa, L.; Leroy, O.; Dragoe, D.; Bruzaud, J.; Herry, J.M.; Guilbaud, M.; Bellon-Fontaine, M.N.; Roger, P. Antibacterial poly(ethylene terephthalate) surfaces obtained from thymyl methacrylate polymerization. *J. Polym. Sci. Part A Polym. Chem.* **2015**, *53*, 1975–1985. [CrossRef]
24. Xv, J.; Li, H.; Zhang, W.; Lai, G.; Xue, H.; Zhao, J.; Tu, M.; Zeng, R. Anti-biofouling and functionalizable bioinspired chitosan-based hydrogel coating via surface photo-immobilization. *J. Biomater. Sci. Polym. Ed.* **2019**, *30*, 398–414. [CrossRef]
25. Gao, F.; Jiang, M.; Liang, W.; Fang, X.; Bai, F.; Zhou, Y.; Lang, M. Co-electrospun cellulose diacetate-graft-poly(ethylene terephthalate) and collagen composite nanofibrous mats for cells culture. *J. Appl. Polym. Sci.* **2020**, *137*, 49350. [CrossRef]
26. Gun Gok, Z.; Inal, M.; Bozkaya, O.; Yigitoglu, M.; Vargel, I. Production of 2-hydroxyethyl methacrylate-g-poly(ethylene terephthalate) nanofibers by electrospinning and evaluation of the properties of the obtained nanofibers. *J. Appl. Polym. Sci.* **2020**, *137*, 9257. [CrossRef]
27. Olson, R.A.; Korpusik, A.B.; Sumerlin, B.S. Enlightening advances in polymer bioconjugate chemistry: Light-based techniques for grafting to and from biomacromolecules. *Chem. Sci.* **2020**, *11*, 5142–5156. [CrossRef]
28. Zhang, S.; Ding, F.; Wang, Y.; Ren, X.; Huang, T.S. Antibacterial and Hydrophilic Modification of PET Fabrics by Electron Beam Irradiation Process. *Fibers Polym.* **2020**, *21*, 1023–1031. [CrossRef]
29. Coen, M.C.; Lehmann, R.; Groening, P.; Schlapbach, L. Modification of the micro- and nanotopography of several polymers by plasma treatments. *Appl. Surf. Sci.* **2003**, *207*, S0169–S4332.
30. Inagaki, N.; Narushim, K.; Tuchida, N.; Miyazaki, K. Surface characterization of plasma-modified poly(ethylene terephthalate) film surfaces. *J. Polym. Sci. Part B Polym. Phys.* **2004**, *42*, 3727–3740. [CrossRef]
31. Chung, K.K.; Schumacher, J.F.; Sampson, E.M.; Burne, R.A.; Antonelli, P.J.; Brennan, A.B. Impact of engineered surface microtopography on biofilm formation of Staphylococcus aureus. *Biointerphases* **2007**, *2*, 89–94. [CrossRef]
32. Yang, L.; Chen, J.; Guo, Y.; Zhang, Z. Surface modification of a biomedical polyethylene terephthalate (PET) by air plasma. *Appl. Surf. Sci.* **2009**, *255*, 4446–4451. [CrossRef]
33. Khoffi, F.; Khalsi, Y.; Chevrier, J.; Kerdjoud, J.H.; Tazibt, A.; Heim, F. Surface modification of polymer textile biomaterials by N2 supercritical jet: Preliminary mechanical and biological performance assessment. *J. Mech. Behav. Biomed. Mater.* **2020**, *107*, 103772. [CrossRef]

34. Del Hoyo-Gallego, S.; Pérez-Álvarez, L.; Gómez-Galván, F.; Lizundia, E.; Kuritka, I.; Sedlarik, V.; Laza, J.M.; Vila-Vilela, J.L. Construction of antibacterial poly(ethylene terephthalate) films via layer by layer assembly of chitosan and hyaluronic acid. Carbohydr. *Polymers* **2016**, *143*, 35–43. [CrossRef]
35. Gun Gok, Z.; Gunay, K.; Arslan, M.; Yigitoglu, M.; Vargel, I. Coating of modified poly(ethylene terephthalate) fibers with sericin-capped silver nanoparticles for antimicrobial application. *Polym. Bull.* **2020**, *77*, 1649–1665. [CrossRef]
36. Junthip, J.; Tabary, N.; Maton, M.; Ouerghemmi, S.; Staelens, J.N.; Cazaux, F.; Neut, C.; Blanchemain, N.; Martel, B. Release-killing properties of a textile modified by a layer-by-layer coating based on two oppositely charged cyclodextrin polyelectrolytes. *Int. J. Pharm.* **2020**, *587*, 119730. [CrossRef] [PubMed]
37. Naeem, M.; Felipe, M.B.M.C.; de Medeiros, S.R.B.; Costa, T.H.C.; Libório, M.S.; Alves, C., Jr.; Nascimento, R.M.; Nascimento, I.O.; Sousa, R.R.M.; Feitor, M.C. Novel antibacterial silver coating on PET fabric assisted with hollow-cathode glow discharge. *Polym. Adv. Technol.* **2020**, *31*, 2896–2905. [CrossRef]
38. Rodríguez-Alba, E.; Dionisio, N.; Pérez-Calixto, M.; Huerta, L.; García-Uriostegui, L.; Hautefeuille, M.; Vázquez-Victorio, G.; Burillo, G. Surface modification of polyethylenterephthalate film with primary amines using gamma radiation and aminolysis reaction for cell adhesion studies. *Radiat. Phys. Chem.* **2020**, *176*, 109070. [CrossRef]
39. Sreeja, S.; Muraleedharan, C.V.; Varma, P.R.H.; Sailaja, G.S. Surface-transformed osteoinductive polyethylene terephthalate scaffold as a dual system for bone tissue regeneration with localized antibiotic delivery. *Mater. Sci. Eng. C* **2020**, *109*, 110491. [CrossRef] [PubMed]
40. Samipour, S.; Taghvaei, H.; Mohebbi-Kalhori, D.; Rahimpour, M.R. Plasma treatment and chitosan coating: A combination for improving PET surface properties. *Surf. Innov.* **2020**, *8*, 76–88. [CrossRef]
41. Jung, K.H.; Huh, M.W.; Meng, W.; Yuan, J.; Hyun, S.H.; Bae, J.S.; Hudson, S.M.; Kang, I.-K. Preparation and antibacterial activity of PET/chitosan nanofibrous mats using an electrospinning technique. *J. Appl. Polym. Sci.* **2007**, *105*, 2816–2823. [CrossRef]
42. Masoomi, M.; Tavangar, M.; Razavi, S.M.R. Preparation and investigation of mechanical and antibacterial properties of poly(ethylene terephthalate)/chitosan blend. *RSC Adv.* **2015**, *5*, 79200–79206. [CrossRef]
43. Jou, C.H.; Yuan, L.; Lin, S.-M.; Hwang, M.C.; Chou, W.L.; Yu, D.-G.; Yang, M.-C. Biocompatibility and antibacterial activity of chitosan and hyaluronic acid immobilized polyester fibers. *J. Appl. Polym. Sci.* **2007**, *104*, 220–225. [CrossRef]
44. Pérez-Álvarez, L.; Ruiz-Rubio, L.; Azua, I.; Benito, V.; Bilbao, A.; Vilas-Vilela, J.L. Development of multiactive antibacterial multilayers of hyaluronic acid and chitosan onto poly(ethylene terephthalate). *Eur. Polym. J.* **2019**, *112*, 31–37. [CrossRef]
45. Gahtan, V.; Esses, G.E.; Bandyk, D.F.; Nelson, R.T.; Dupont, E.; Mills, J.L. Antistaphylococcal activity of rifampin-bonded gelatin-impregnated dacron grafts. *J. Surgical. Res.* **1995**, *58*, 105–110. [CrossRef] [PubMed]
46. Bucheńska, J.; Slomkowski, S.; Tazbir, J.; Sobolewska, E. Antibacterial poly(ethylene terephthalate) yarn containing cephalosporin type antibiotic. *Fibres Text. East. Eur.* **2003**, *11*, 41–47.
47. Ginalska, G.; Osinska, M.; Uryniak, A.; Urbanik-Sypniewska, T.; Belcarz, A.; Rzeski, W.; Wolski, A. Antibacterial activity of gentamicin-bonded gelatin-sealed polyethylene terephthalate vascular prostheses. *Eur. J. Vasc. Endovasc. Surg.* **2005**, *29*, 419–424. [CrossRef]
48. Shimanovich, U.; Cavaco-Paulo, A.; Nitzan, Y.; Gedanken, A. Sonochemical coating of cotton and polyester fabrics with "antibacterial" BSA and casein spheres. *Chem. Eur. J.* **2012**, *18*, 365–369. [CrossRef] [PubMed]
49. Aubert-Viard, F.; Mogrovejo-Valdivia, A.; Tabary, N.; Maton, M.; Chai, F.; Neut, C.; Martel, B.; Blanchemain, N. Evaluation of antibacterial textile covered by layer-by-layer coating and loaded with chlorhexidine for wound dressing application. *Mater. Sci. Eng. C* **2019**, *100*, 554–563. [CrossRef]
50. Salmoukas, C.; Ruemke, S.; Rubalskii, E.; Burgwitz, K.; Haverich, A.; Kuehn, C. Vascular graft pre-treatment with daptomycin prior to implantation prevents graft infection with *Staphylococcus aureus* in an in vivo model. *Surg. Infect.* **2020**, *21*, 161–168. [CrossRef] [PubMed]
51. Levy, S.B.; Marshall, B. Antibacterial resistance worldwide: Causes, challenges and responses. *Nat. Med.* **2004**, *10*, 122–129. [CrossRef]
52. Medici, S.; Peana, M.; Nurchi, V.M.; Lachowicz, J.I.; Crisponi, G.; Zoroddu, M.A. Noble metals in medicine: Latest advances. *Coord. Chem. Rev.* **2015**, *284*, 329–350. [CrossRef]
53. Paladini, F.; Pollini, M.; Sannino, A.; Ambrosio, L. Metal-based antibacterial substrates for biomedical applications. *Biomacromolecules* **2015**, *16*, 1873–1885. [CrossRef]

54. Giannousi, K.; Pantazaki, A.; Dendrinou-Samara, C. bnjmpper-Based Nanoparticles as Antimicrobials. In *Nanostructures for Antimicrobial Therapy: Nanostructures in Therapeutic*; Ficai, A., Grumezescu, A.M., Eds.; Elsevier Inc.: Amsterdam, The Netherlands, 2017; Chapter 23; pp. 515–529, ISBN 9780323461511.
55. Chuang, K.T.; Abdullah, H.; Leu, S.J.; Cheng, K.; Bin Kuo, D.H.; Chen, H.C.; Chien, J.H.; Hu, W.T. Metal oxide composite thin films made by magnetron sputtering for bactericidal application. *J. Photochem. Photobiol. A Chem.* **2017**, *337*, 151–164. [CrossRef]
56. Hoseinzadeh, E.; Makhdoumi, P.; Taha, P.; Hossini, H.; Stelling, J.; Kamal, M.A.; Ashraf, G. A review on nano-antimicrobials: Metal nanoparticles, methods and mechanisms. *Curr. Drug Metab.* **2017**, *18*, 120–128. [CrossRef] [PubMed]
57. Slavin, Y.N.; Asnis, J.; Häfeli, U.O.; Bach, H. Metal nanoparticles: Understanding the mechanisms behind antibacterial activity. *J. Nanobiotechnol.* **2017**, *15*, 65. [CrossRef] [PubMed]
58. Klebowski, B.; Depciuch, J.; Parlinska-Wojtan, M.; Baran, J. Applications of noble metal-based nanoparticles in medicine. *Int. J. Mol. Sci.* **2018**, *19*, 4031. [CrossRef] [PubMed]
59. Sánchez-López, E.; Gomes, D.; Esteruelas, G.; Bonilla, L.; Lopez-Machado, A.L.; Galindo, R.; Cano, A.; Espina, M.; Ettecheto, M.; Camins, A.; et al. Metal-based nanoparticles as antimicrobial agents: An overview. *Nanomaterials* **2020**, *10*, 292. [CrossRef]
60. Tweden, K.S.; Cameron, J.D.; Razzouk, A.J.; Bianco, RW.; Holmberg, W.R.; Bricault, RJ.; Barry, J.E.; Tobin, E. Silver modification of polyethylene terephthalate textiles for antimicrobial protection. *ASAIO J.* **1997**, *43*, 475–481. [CrossRef]
61. Perelshtein, I.; Applerot, G.; Perkas, N.; Guibert, G.; Mikhailov, S.; Gedanken, A. Sonochemical coating of silver nanoparticles on textile fabrics (nylon, polyester and cotton) and their antibacterial activity. *Nanotechnology* **2008**, *19*, 245705. [CrossRef]
62. Radetić, M.; Ilić, V.; Vodnik, V.; Dimitricjevic, S.; Jovanovic, P.; Šaponjić, Z.; Nedeljković, J.M. Antibacterial effect of silver nanoparticles deposited on corona-treated polyester and polyamide fabrics. *Polym. Adv. Technol.* **2008**, *19*, 1816–1821. [CrossRef]
63. Gorenšek, M.; Gorjanc, M.; Bukošek, V.; Kovac, J.; Jovančić, P.; Mihailović, D. Functionalization of PET fabrics by corona and nano silver. *Text. Res. J.* **2010**, *80*, 253–262. [CrossRef]
64. Chen, Y.H.; Hsu, C.C.; He, J.L. Antibacterial silver coating on poly(ethylene terephthalate) fabric by using high power impulse magnetron sputtering. *Surf. Coat. Technol.* **2013**, *232*, 868–875. [CrossRef]
65. Kumar, V.; Jolivalt, C.; Pulpytel, J.; Jafari, R.; Arefi-Khonsari, F. Development of silver nanoparticle loaded antibacterial polymer mesh using plasma polymerization process. *J. Biomed. Mater. Res. Part A* **2013**, *101*, 1121–1132. [CrossRef]
66. Majumdar, A.; Butola, B.S.; Thakur, S. Development and performance optimization of knitted antibacterial materials using polyester-silver nanocomposite fibres. *Mater. Sci. Eng. C* **2015**, *54*, 26–31. [CrossRef] [PubMed]
67. Nguyenova, H.Y.; Vokata, B.; Zaruba, K.; Siegel, J.; Kolska, Z.; Svorcik, V.; Slepicka, P.; Reznickova, A. Silver nanoparticles grafted onto PET: Effect of preparation method on antibacterial activity. *React. Funct. Polym.* **2019**, *145*, 104376. [CrossRef]
68. Li, J.X.; Wang, J.; Shen, L.R.; Xu, ZJ.; Li, P.; Wan, G.J.; Huang, N. The influence of polyethylene tere-phthalate surfaces modified by silver ion implantation on bacterial adhesion behaviour. *Surf. Coat. Technol.* **2007**, *201*, 8155–8159. [CrossRef]
69. Rajabi, A.; Ghazali, M.J.; Mahmoudi, E.; Baghdadi, A.H.; Mohammad, A.W.; Mustafah, N.M.; Ohnmar, H.; Naicker, A.S. Synthesis, characterization, and antibacterial activity of Ag_2O-loaded polyethylene terephthalate fabric via ultrasonic method. *Nanomaterials* **2019**, *9*, 450. [CrossRef] [PubMed]
70. Mihailović, D.; Šaponjić, Z.; Radoičić, M.; Radetic, T.; Jovancic, P.; Nedeljković, J.; Radetić, M. Functionalization of polyester fabrics with alginates and TiO2 nanoparticles. *Carbohyd. Polym.* **2010**, *79*, 526–532. [CrossRef]
71. Mihailović, D.; Šaponjić, Z.; Molina, R.; Radoičić, M.; Esquena, J.; Jovančić, P.; Nedeljković, J.; Radetić, M. Multifunctional properties of polyester fabrics modified by corona discharge/air RF plasma and colloidal TiO2 nanoparticles. *Polym. Compos.* **2011**, *32*, 390–397. [CrossRef]
72. Xu, Y.; Wen, W.; Wu, J.M. Titania nanowires functionalized polyester fabrics with enhanced photocatalytic and antibacterial performances. *J. Hazard. Mater.* **2018**, *343*, 285–297. [CrossRef]

73. Touhid, S.S.B.; Shawon, M.R.K.; Khoso, N.A.; Xu, Q.; Pan, D.; Liu, X. TiO2/Cu composite NPs coated polyester fabric for the enhancement of antibacterial durability. IOP Conf. *Ser. Mater. Sci. Eng.* **2020**, *774*, 012114. [CrossRef]
74. Deng, B.; Yan, X.; Wei, Q.; Gao, W. AFM characterization of nonwoven material functionalized by ZnO sputter coating. *Mater. Charact.* **2007**, *58*, 854–858. [CrossRef]
75. Fiedot-Toboła, M.; Ciesielska, M.; Maliszewska, I.; Rac-Rumiejowska, O.; Suchorska-Woźniak, P.; Teterycz, H.; Bryjak, M. Deposition of zinc oxide on different polymer textiles and their antibacterial properties. *Materials* **2018**, *11*, 707. [CrossRef]
76. Yuan, X.; Xu, W.; Huang, F.; Chen, D.; Wei, Q. Polyester fabric coated with Ag/ZnO composite film by magnetron sputtering. *Appl. Surf. Sci.* **2016**, *390*, 863–869. [CrossRef]
77. Weichold, O.; Goel, P.; Lehmann, K.H.; Möller, M. Solvent-crazed PET fibers imparting antibacterial activity by release of Zn2+. *J. Appl. Polym. Sci.* **2009**, *112*, 2634–2640. [CrossRef]
78. Yang, X.; Yang, J.; Wang, L.; Ran, B.; Jia, Y.; Zhang, L.; Yang, G.; Shao, H.; Jiang, X. Pharmaceutical intermediate-modified gold nanoparticles: Against multidrug-resistant bacteria and wound-healing application via an electrospun scaffold. *ACS Nano* **2017**, *11*, 5737–5745. [CrossRef] [PubMed]
79. Chen, Y.H.; Wu, G.W.; He, J.L. Antimicrobial brass coatings prepared on poly(ethylene terephthalate) textile by high power impulse magnetron sputtering. *Mater. Sci. Eng. C* **2015**, *48*, 41–47. [CrossRef]
80. Ahmad, S.; Ashraf, M.; Ali, A.; Shaker, K.; Umair, M.; Afzal, A.; Nawab, Y.; Rasheed, A. Preparation of conductive polyethylene terephthalate yarns by deposition of silver & copper nanoparticles. *Fibres Text. East. Eur.* **2017**, *25*, 25–30. [CrossRef]
81. Nguyen, V.T.; Trinh, K.S. In situ deposition of copper nanoparticles on polyethylene terephthalate filters and antibacterial testing against Escherichia coli and Salmonella enterica. *Braz. J. Chem. Eng.* **2019**, *36*, 1553–1560. [CrossRef]
82. Zhou, J.; Fei, X.; Li, C.; Yu, S.; Hu, Z.; Xiang, H.; Sun, B.; Zhu, M. Integrating Nano-Cu2O@ZrP into in situ polymerized polyethylene terephthalate (PET) fibers with enhanced mechanical properties and antibacterial activities. *Polymers* **2019**, *11*, 113. [CrossRef]
83. Scopus Base. 5212 Documents Results on Antibacterial& Copper. Available online: https://www-1scopus-1com-10000147v00b6.han.p.lodz.pl/results/results.uri?numberOfFields=0&src=s&clickedLink=&edit=&editSaveSearch=&origin=searchbasic&authorTab=&affiliationTab=&advancedTab=&scint=1&menu=search&tablin=&searchterm1=Antibacterial+Copper&field1=TITLE_ABS_KEY&dateType=Publication_Date_Type&yearFrom=Before+1960&yearTo=Present&loadDate=7&documenttype=All&accessTypes=All&resetFormLink=&st1=Antibacterial+Copper&st2=&sot=b&sdt=b&sl=35&s=TITLE-ABS-KEY%28Antibacterial+Copper%29&sid=7456a8ca6e782e4746a73fa9c19ff5e7&searchId=7456a8ca6e782e4746a73fa9c19ff5e7&txGid=271a497002bc4a7ce75a80cc22cd9308&sort=plf-f&originationType=b&rr= (accessed on 10 September 2020).
84. Khodashenas, B.; Ghorbani, H.R. Synthesis of copper nanoparticles: An overview of the various methods. *Korean J. Chem. Eng.* **2014**, *31*, 1105–1109. [CrossRef]
85. Camacho-Flores, B.A.; Martínez-Álvarez, O.; Arenas-Arrocena, M.C.; Garcia-Contreras, R.; Argueta-Figueroa, L.; de la Fuente-Hernández, J.; Acosta-Torres, L.S. Copper: Synthesis techniques in nanoscale and powerful application as an antimicrobial agent. *J. Nanomater.* **2015**, 415238. [CrossRef]
86. Rafique, M.; Shaikh, A.J.; Rasheed, R.; Tahir, M.B.; Bakhat, H.F.; Rafique, M.S.; Rabbani, F. A review on synthesis, characterization and applications of copper nanoparticles using green method. *Nanomaterials* **2017**, *12*, 1750043. [CrossRef]
87. Grass, G.; Rensing, C.; Solioz, M. Metallic copper as an antimicrobial surface. *Appl. Environ. Microbiol.* **2011**, *77*, 1541–1547. [CrossRef] [PubMed]
88. Radetzki, M. Seven thousand years in the service of humanity—The history of copper, the red metal. *Resour. Policy* **2009**, *34*, 176–184. [CrossRef]
89. Barceloux, D.G. Copper. *Clin. Toxicol.* **1999**, *37*, 217–230. [CrossRef] [PubMed]
90. Hans, M.; Erbe, A.; Mathews, S.; Chen, Y.; Solioz, M.; Mücklich, F. Role of copper oxides in contact killing of bacteria. *Langmuir* **2013**, *29*, 16160–16166. [CrossRef]
91. Hans, M.; Mathews, S.; Mucklich, F.; Solioz, M. Physicochemical properties of copper important for its antibacterial activity and development of a unified model. *Biointerphases* **2016**, *11*, 018902. [CrossRef]

92. Ingle, A.P.; Duran, N.; Rai, M. Bioactivity, mechanism of action, and cytotoxicity of copper-based nanoparticles: A review. *Appl. Microbiol. Biotechnol.* **2014**, *98*, 1001–1009. [CrossRef]
93. Dalecki, A.G.; Crawford, C.L.; Wolschendorf, F. Copper and antibiotics: Discovery, modes of action, and opportunities for medicinal applications. *Adv. Microb. Physiol.* **2017**, *70*, 193–260. [CrossRef]
94. Vincent, M.; Duval, R.E.; Hartemann, P.; Engels-Deutsch, M. Contact killing and antimicrobial properties of copper. *J. Appl. Microbiol.* **2018**, *124*, 1032–1046. [CrossRef]
95. Fowler, L.; Engqvist, H.; Öhman-Mägi, C. Effect of copper ion concentration on bacteria and cells. *Materials* **2019**, *12*, 3798. [CrossRef]
96. Bastos, C.A.P.; Faria, N.; Wills, J.; Malmberg, P.; Scheers, N.; Rees, P.; Powell, J.J. Copper nanoparticles have negligible direct antibacterial impact. *NanoImpact* **2020**, *17*, 100192. [CrossRef]
97. Kobayashi, Y.; Yasuda, Y.; Morita, T. Recent advances in the synthesis of copper-based nanoparticles for metal-metal bonding processes. *J. Sci. Adv. Mater. Devices* **2016**, *1*, 413–430. [CrossRef]
98. Fernández-Arias, M.; Boutinguiza, M.; del Val, J.; Riveiro, A.; Rodriguez, D.; Arias-Gonzalez, F.; Gil, J.; Pou, J. Fabrication and deposition of copper and copper oxide nanoparticles by laser ablation in open air. *Nanomaterials* **2020**, *10*, 300. [CrossRef] [PubMed]
99. Wei, Q.; Xiao, X.; Hou, D.; Ye, H.; Huang, F. Characterization of nonwoven material functionalized by sputter coating of copper. *Surf. Coat. Technol.* **2008**, *202*, 2535–2539. [CrossRef]
100. Segura, G.; Guzmán, P.; Zuñiga, P.; Chaves, S.; Barrantes, Y.; Navarro, G.; Asenjo, J.; Guadamuz, S.; Vargas, V.I.; Chaves, J. Copper deposition on fabrics by rf plasma sputtering for medical applications. *J. Phys. Conf. Ser.* **2015**, *591*, 012046. [CrossRef]
101. Tan, X.Q.; Liu, J.Y.; Niu, J.R.; Liu, J.Y.; Tian, J.Y. Recent progress in magnetron sputtering technology used on fabrics. *Materials* **2018**, *11*, 1953. [CrossRef]
102. Kudzin, Z.H.; Kudzin, M.H.; Drabowicz, J.; Stevens, C.V. Aminophosphonic acids-phosphorus analogues of natural amino acids. Part 1: Syntheses of α-aminophosphonic acids. *Curr. Org. Chem.* **2011**, *15*, 2015–2071. [CrossRef]
103. Kudzin, Z.H.; Depczyński, R.; Kudzin, M.H.; Łuczak, J.; Drabowicz, J. 1-(N-Trifluoroacetylamino) alkylphosphonic acids: Synthesis and properties. *Amino Acids* **2007**, *33*, 663–667. [CrossRef]
104. Kudzin, M.H.; Mrozińska, Z.; Walawska, A.; Sójka-Ledakowicz, J. Biofunctionalization of textile materials. 1. Biofunctionalization of poly(propylene) (PP) nonwovens fabrics by Alafosfalin. *Coatings* **2019**, *9*, 412. [CrossRef]
105. Kudzin, M.H.; Mrozińska, Z. Biofunctionalization of textile materials. 2. Antimicrobial modification of poly(lactide) (PLA) nonwoven fabrics by fosfomycin. *Polymers* **2020**, *12*, 768. [CrossRef]
106. Kudzin, M.H.; Mrozińska, Z. Biofunctionalization of textile materials. 3. Biofunctionalization of poly(lactide) (PLA) nonwovens fabrics by KI. *Coatings* **2020**, *10*, 593. [CrossRef]
107. Shahidi, S.; Ghoranneviss, M.; Moazzenchi, B.; Rashidi, A.; Mirjalili, M. Investigation of antibacterial activity on cotton fabrics with cold plasma in the presence of a magnetic field. Plasma Process. *Polymers* **2007**, *4*, 1098–1103.
108. Badaraev, A.D.; Nemoykina, A.L.; Bolbasov, E.N.; Tverdokhlebov, S.I. PLLA scaffold modification using magnetron sputtering of the copper target to provide antibacterial properties. *Res. Technol.* **2017**, *3*, 204–211. [CrossRef]
109. Gorberg, B.L.; Ivanov, A.A.; Mamontov, O.V.; Stegnin, V.A.; Titov, V.A. Modification of textile materials by the deposition of nanocoatings by magnetron ion-plasma sputtering. *Russ. J. Gen. Chem.* **2013**, *83*, 157–163. [CrossRef]
110. Locatelli, P.; Woutters, S.; Lindsay, C.; Schreder, S.L.M.; Hobdell, J.H.; Saian, A. Synthesis of polyurea–polyether nanoparticles via spontaneous nanoprecipitation. *RSC Adv.* **2015**, *5*, 41668. [CrossRef]
111. Kudzin, M.H.; Mrozińska, Z.; Kaczmarek, A.; Lisiak-Kucińska, A. Deposition of Copper on Poly(Lactide) Non-Woven Fabrics by Magnetron Sputtering–Fabrication of New Multi-Functional, Antimicrobial Composite. *Materials* **2020**, *13*, 3971. [CrossRef]
112. ISO 15632:2012. *Microbeam Analysis–Selected Instrumental Performance Parameters for the Specification and Checking of Energy-Dispersive X-ray Spectrometers for Use in Electron Probe Microanalysis*; International Organization for Standardization: Geneva, Switzerland, 2012.
113. *Analytical Methods for Atomic Absorption Spectroscopy*; The Perkin-Elmer Corporation, 1996; Volume 46, Available online: www.perkinelmer.com (accessed on 3 July 2020).

114. EN 137581:2002. *Textiles. Solar UV Protective Properties. Method of Test for Apparel Fabrics*; International Organization for Standardization: Geneva, Switzerland, 2002.
115. EN ISO 9237:1998. *Textiles. Determination of the Permeability of Fabrics to Air*; International Organization for Standardization: Geneva, Switzerland, 1998.
116. EN ISO 10319:2015. *Geosynthetics–Wide-Width Tensile Test*; International Organization for Standardization: Geneva, Switzerland, 2015.
117. EN ISO 5084:1999. *Textiles–Determination of Thickness of Textiles and Textile Products*; International Organization for Standardization: Geneva, Switzerland, 1999.
118. EN ISO 11092:20141–1. *Textiles–Physiological Effects–Measurement of Thermal and Water-Vapour Resistance Under Steady-State Conditions*; International Organization for Standardization: Geneva, Switzerland, 2014.
119. EN ISO 20645:2006. *Textile Fabrics. Determination of Antibacterial Activity—Agar Diffusion Plate Test*; International Organization for Standardization: Geneva, Switzerland, 2006.
120. PN EN 14119: 2005 Testing of Textiles. *Evaluation of the Action of Microfungi. Visual Method*; International Organization for Standardization: Geneva, Switzerland, 2005.
121. Gong, H.; Ozgen, B. Engineering of High-Performance Textiles. 5–Fabric structures: Woven, knitted, or nonwoven. *Text. Inst. Book Ser.* **2018**, 107–131. [CrossRef]
122. Legois, Y.; Aucouturier, M.; Ollivier, E.; Darque-Ceretti, E.; Macheto, P. Adhesion mechanism of copper films deposited by magnetron sputtering on polyamide composites. *Surf. Eng.* **1998**, *14*, 259–264. [CrossRef]
123. Ringenbach, A.; Jugnet, Y.; Duc, T.M. Interfacial Chemistry in Al and Cu metallization of untreated and plasma treated polyethylene and polyethyleneterephthalate. *J. Adhes. Sci. Technol.* **1995**, *9*, 1209–1228. [CrossRef]
124. Gollier, P.A.; Bertrand, P. Diffusion of copper in polymer during the metallization of PET. *J. Adhesion.* **1996**, *58*, 173–182. [CrossRef]
125. Bertrand, P.; Lambert, P.; Travaly, Y. Polymer metallization: Low energy ion beam surface modification to improve adhesion. *Nucl. Instr. Meth. Phys. Res. B* **1997**, *131*, S0168–S0583. [CrossRef]
126. Zhu, Z.; Kelley, M.J. Poly(ethylene terephthalate) surface modification by deep UV (172 nm) irradiation. *Appl. Surf. Sci.* **2004**, *236*, 416–425. [CrossRef]
127. Zhu, Z.; Kelley, M.J. Effect of deep UV (172 nm) irradiation on PET: ToF/SIMS analysis. *Appl. Surf. Sci.* **2004**, *231*, 302–308. [CrossRef]
128. Teng, C.; Yu, M. Preparation and property of poly(ethylene terephthalate) fibers providing ultraviolet radiation protection. *J. Appl. Polym. Sci.* **2003**, *88*, 1180–1185. [CrossRef]
129. Dimitrovski, K.; Sluga, F.; Urbas, R. Evaluation of the structure of monofilament PET woven fabrics and their UV protection properties. *Text. Res. J.* **2010**, *80*, 1027–1037. [CrossRef]
130. Urbas, R.; Sluga, F.; Miljković, J.; Bartenjev, I. Comparison of in vitro and in vivo ultraviolet protective properties of PET textile samples. *Acta Dermatovener. APA* **2012**, *21*, 11–14.
131. Bunsell, A.R. *Handbook of Properties of Textile and Technical Fibres*; Elsevier Ltd.: Amsterdam, The Netherlands, 2018.